Title

A Vault-Encapsulated Enzyme Approach for Efficient Degradation and Detoxification of Bisphenol A and Its Analogues

Journal

ACS Sustainable Chemistry & Engineering, 7(6)

ISSN

2168-0485

Authors

Wang, Meng

Chen, Yichang

Kickhoefer, Valerie A

et al.

Publication Date

2019-03-18

DOI

10.1021/acssuschemeng.8b05432

Peer reviewed

Published in final edited form as:

ACS Sustain Chem Eng. 2019 March 18; 7(6): 5808–5817. doi:10.1021/acssuschemeng.8b05432.

A Vault-Encapsulated Enzyme Approach for Efficient Degradation and Detoxification of Bisphenol A and Its Analogues

Meng Wang[†,▽], **Yichang Chen**[‡,▽], **Valerie A. Kickhoefer**[§,‖], **Leonard H. Rome**[§,⊥], **Patrick Allard**[‡,#], **Shaily Mahendra**[*,†,‡,⊥]

[†]Department of Civil and Environmental Engineering, University of California, Los Angeles, 420 Westwood Plaza, Los Angeles, California 90095, United States

[‡]Molecular Toxicology Interdepartmental Program, University of California, Los Angeles, 650 Charles E Young Drive South, Los Angeles, California 90095, United States

[§]Department of Biological Chemistry, University of California, Los Angeles, 615 Charles E Young Drive South, Los Angeles, California 90095, United States

[‖]Vault Nano Inc., 570 Westwood Plaza, Los Angeles, California 90095, United States

[⊥]California Nanosystems Institute, University of California, Los Angeles, 570 Westwood Plaza, Los Angeles, California 90095, United States

[#]Institute for Society & Genetics, University of California, Los Angeles, 621 Charles E Young Drive South, Los Angeles, California 90095, United States

Abstract

We report an effective and environmentally sustainable water treatment approach using enzymes encapsulated in biogenic vault nanoparticles. Manganese peroxidase (MnP), whose stability was remarkably extended by encapsulating into vaults, rapidly catalyzed the biotransformation of endocrine-disrupting compounds, including bisphenol A (BPA), bisphenol F (BPF), and bisphenol AP (BPAP). The vault-encapsulated MnP (vMnP) treatment removed 80–95% of each of the tested bisphenols (BPs) at lower enzyme dosage, while free native MnP (nMnP) only resulted in a 19–36% removal, over a 24-h period. Treatment by vMnP and nMnP resulted in considerable disparities in product species and abundance, which were consistent with the observed changes in the estrogenic activities of BPs. To test if vMnP-catalyzed transformations generated toxic intermediates, we assessed biological hallmarks of BP toxicity, namely, the ability to disrupt reproductive processes. The toxicity of vMnP-treated samples, as measured in the

[*]**Corresponding Author:** mahendra@seas.ucla.edu.
[▽]Contributed equally to this work.

Supporting Information

The Supporting Information is available free of charge on the ACS Publications website at DOI: 10.1021/acssusche-meng.8b05432. Experimental details on product profile characterizations, HPLC analysis, and SPE procedure; physical properties of BPs; vault structure; schematic of vault encapsulation; removal kinetics and MnP-mediated transformation pathways of BPs; effects of ethanol vehicle on reproductive features; larval lethality and estrogenic activity of BPs and their degradation products (PDF)

The authors declare the following competing financial interest(s): V.A.K. and L.H.R. have financial interest in Vault Nano Inc., which has licensed intellectual property used in this study from the Regents of the University of California.

model organism, *Caenorhabditis elegans*, was dramatically reduced for all three BPs, including the reproductive indicators of BPA exposure such as reduced fertility and increased germ cell death. Collectively, our results indicate that the vMnP system represents an efficient and safe approach for the removal of BPs and promise the development of vault-encapsulated customized enzymes for treating other targeted organic compounds in contaminated waters.

Graphical Abstract

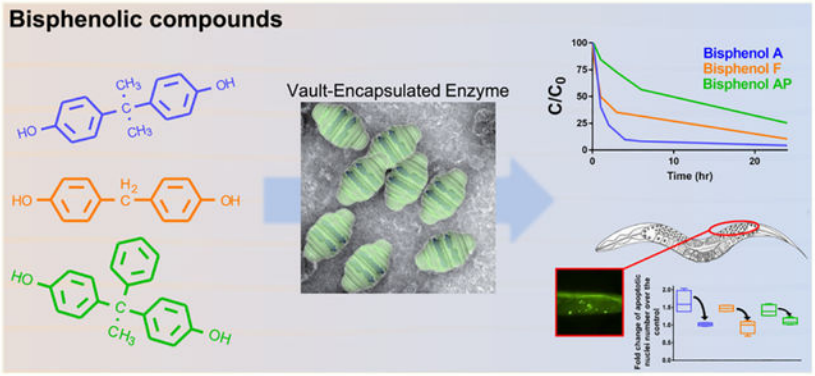

Keywords

White-rot fungus; Ligninolytic; Biodegradation; Entrapment; Estrogenic

INTRODUCTION

Enzymatic bioremediation, which utilizes enzymatic catalysis to degrade or transform contaminants in the environment, has been explored for several decades.[1–4] Benefiting from high efficiency and specificity of enzymes, enzymatic treatment is therefore considered effective and, because of its reduced chemical and energy use, congruent with the principles of environmental sustainability.[1,4,5] However, as many enzymes are not stable outside living cells, and can be inactivated by heat, cocontaminants, and products formed by their own activities, the use of enzymes in water treatment requires high dosage and frequent replenishment, which raises the cost and limits their applications in large scale systems.[1] A potential solution is to entrap enzymes in solid supports, such as alginate beads, hollow fiber membranes, and magnetic particles,[1] to lower dosage and prevent inactivation, thus reducing the cost. But entrapped enzymes usually become less active due to substrate diffusion resistance caused by the solid supports.[1,5,6] Recent advances in nanotechnology have provided a wide variety of nanomaterials that are potential alternatives to conventional entrapment supports. Owing to their small dimensions, substrate diffusion problems can be minimized in nanoimmoblization, which benefit enzyme catalytic efficiency.[5,6] However, many of these materials, such as carbon nanotubes, polymeric nanoparticles, and mesoporous metal oxides, require harsh synthesis conditions and complex support preparation and immobilization protocols and also cause cytotoxicity and possess potential human health risks, which limit their use in environmental applications, particularly in water treatment.[6]

The use of bionanomaterials in enzyme stabilization is gaining more attention, as they are more biocompatible and synthesized under physiological conditions.[7] We recently reported a protein scaffold based stabilization approach by encapsulating enzymes in vault nanoparticles.[8] Vaults are the largest natural ribonucleoprotein particles with dimensions of 41 × 41 × 72.5 nm, which are synthesized in humans and most other eukaryotes.[9] Each native vault consists of 78 copies of major vault protein (MVP), which assemble into the outer shell of the particle, and several copies of two different vault-associated proteins and small untranslated RNAs.[9] Synthesized from heterologously expressed MVP in insect or yeast cells, recombinant vaults are empty protein shells that are morphologically identical to native vault particles with core cavities of around 3.87×10^4 nm^3 (Figure S1).[10,11] Such large scaffolds not only protect encapsulated proteins from deactivators but also allow free enzyme conformational changes that are required for proper catalytic cycles, enabling vaults to be plausible carriers for immobilizing and stabilizing enzymes.[7] The INT domain, a protein sequence that was derived from one of the vault-associated proteins, has a strong noncovalent interaction with vault interior binding sites and is used to direct fusion proteins into vaults.[12] Due to such specific interaction, INT-tagged enzymes can be selectively taken up by vaults from complex matrix materials, which potentially obviates the need of pre-enzyme purification and concentration prior to immobilization and provide a simple and low-cost immobilization methodology. Our recent study demonstrated that the vault-encapsulated manganese peroxidase (MnP) exhibited better storage stability and higher resistance against heat inactivation than free MnP,[8,11] whereas the effectiveness of vault encapsulation toward enhancing enzymatic treatment of various water contaminants is still unknown.

Bisphenol A (BPA, Table S1), a chemical commonly used in plastic, paper, and food packaging industries, is one of the most prevalent endocrine disrupting compounds (EDCs) in the environment.[13] A large number of studies have epidemiologically and mechanistically linked BPA exposure to a variety of significant adverse health effects including, most notably, a strong impact on reproduction and fertility.[14] In recent years, these health risk concerns associated with its exposure have led to a substitution of BPA with its structural analogues (Table S1), such as bisphenol F (BPF), bisphenol S (BPS), and bisphenol AP (BPAP). BPF shares the highest structural relationship with BPA and shows a similar octanol–water partition coefficient (K_{OW}), pK_a, and water solubility.[15] The more hydrophilic BPS exhibits more than 3 times higher water solubility than BPA, and lower K_{OW} and pK_a.[16] BPAP, the BPA analogue with a phenyl substituted for the methyl group at the quaternary α-carbon, has more than 100 times lower water solubility and higher K_{OW}.[17] These analogues are now being used in numerous commercial products, and consequently, they are now also found in surface water,[18] wastewater,[19] and sediments.[13] However, due to their high degree of structural similarities with BPA, many of these substitutes have been shown to possess similar endocrine disrupting activity and reproductive toxicity as BPA.[20,21]

Several oxidative enzymes, such MnP, horseradish peroxidase, and laccase, have been demonstrated to mediate transformation of BPA via coupling reactions or scission reactions.[2,22] However, similar to many other oxidation processes, enzymatic catalysis does not completely mineralize bisphenols (BPs), leaving a wide range of intermediates.[2,23,24] Since their chemical structure is similar to that of their parent compounds, such

intermediates are also likely to pose health risks, especially reproductive effects, which are considered signatures of BPs' toxicity.[20,25–30] Several studies have assessed the toxicity of BPA oxidative transformation products but focused on acute toxicity only.[23,24] Evaluation of the reproductive toxicity of such intermediates will provide deeper understanding of detoxification processes of BPs and inform the assessment of various remediation strategies.

The aim of this study was to develop a vault-encapsulated enzymatic system as an effective and sustainable approach toward contaminants removal and detoxification. We investigated the transformation of BPA and its analogues BPS, BPF, and BPAP by vault-encapsulated MnP (hereafter vMnP) at low enzyme dosage, and compared it with unencapsulated MnPs. Then, a combination of *in vitro* and *in vivo* assays was used to assess whether the degradation of the parent compound led to the production of transformation products that caused lower estrogenic and reproductive effects.

EXPERIMENTAL SECTION

Preparation and Characterization of vMnP.

Vaults and recombinant MnP-INT (rMnP) were expressed in *Spodoptera frugiperda* (Sf9) insect cells infected with baculoviruses encoding either human MVP or rMnP as previously described.[8] The rMnP was encapsulated in vaults and purified following standard vault processing protocols.[8,31] In brief, cell-free culture media containing secreted rMnP was mixed with empty vault particles and incubated on ice for 30 min. Due to the dynamic structure of vaults and the strong affinity between their interior binding sites and the INT domain, vaults can selectively internalize INT tagged components (rMnP; Figure S2).[9] Subsequently, vMnP was separated from matrix materials and negative stain rMnP through ultracentrifugation. Purified vMnP was fractionated on a 4–15% SDS-PAGE gel and analyzed by Coomassie staining and Western blotting using primary rabbit anti-INT antibody and secondary goat antirabbit IgG (H+L) (IRDye 800CW, LI-COR). Negative-stain transmission electron microscopy (TEM) was then performed to confirm the intactness, shape, and size of encapsulated vault particles. Number-based particle size distributions and zeta potentials of empty and encapsulated vaults were determined using PALS (ZetaPALS, Brookhaven Instruments).

Transformation of BPs.

All BP removal reactions were performed at 25 °C in a shaking incubator at 250 rpm. For each BP, the reactions were performed in pH 4.5 50 mM malonate buffer with native MnP (nMnP), rMnP, or vMnP; 1.5 mM $MnCl_2$; 300 μM H_2O_2; and 150 μM BP. MnP enzyme was dosed at 19.3, 15.3, 23.3, and 23.3 U/L for BPA, BPS, BPF, and BPAP reactions, respectively. The enzyme activity assays were carried out in a pH 4.5 50 mM malonate buffer containing 2 mM $MnCl_2$, 400 μM H_2O_2, and 100 μM 2,2′-azino-bis(3-ethylbenzothiazoline-6-sulfonic acid) (ABTS). Absorbance increases at 420 nm were recorded for 30 s with a 2 s interval for calculating initial ABTS oxidation rates. Enzyme free conditions were included to correct for any nonenzymatic losses of BPs. To evaluate the contribution of adsorption on vaults to the removal of BPs, vault-only conditions with final concentrations of 1 mg/mL vaults were also tested. At each prespecified time point,

triplicate samples were terminated by adding three volumes of methanol, followed by filtration through 0.2 μm syringe filters. The residual BP concentrations were measured using an HPLC as described in the SI. BPA removal was also tested at pH values ranging from 4.0 to 5.5 with a gradient of pH 0.5. Reaction mixtures were set up as described above in 50 mM malonate buffers at various pH's, each with an initial enzyme activity of 15.3 U/L. Triplicate samples were collected at 0 and 24 h and analyzed using HPLC.

Characterization of Products.

Eleven-milliliter reactions in pH 4.5 50 mM malonate buffers, containing 4.97×10^{-2} μM MnP (vMnP or nMnP), 1.5 mM $MnCl_2$, 300 μM H_2O_2, and 150 μM BP (BPA, BPF, or BPAP), were incubated at 25 °C and at 250 rpm. Matrix tests containing all components except for MnP and BPs were performed as background negative controls, and enzyme-free assays containing all components except for MnP were performed as positive controls. Recoveries of BPA, BPF, and BPAP were also evaluated in the system only containing malonate buffer and 150 μM of BP (Table S2). After a 24-h reaction, 1 mL of solution was collected from each sample and mixed with 2 mL of methanol, and stored prior to determining residual BP concentrations using HPLC. The remaining 10 mL of solution was subjected to solid-phase extraction (SPE) and processed as described in the SI. The final concentrated SPE eluate in 10 μL of ethanol was used for product characterization, estrogen receptor binding assays, and toxicity tests. Two microliters of the final concentrated SPE eluate was diluted in 50 μL of methanol and then subjected to UPLC/MS analyses to characterize and identify transformation products (details in SI). Qualitative and quantitative analyses of UPLC/MS data were carried out using MZmine 2. Detailed data processing methods and parameters are listed in Table S3.

Estrogen Receptor Competitive Binding Assay.

The binding affinities of enzymatically treated BPs toward estrogen receptors α and β were examined using a time-resolved Förster resonance energy transfer (TR-FRET) based ER competitive binding assay at serial dilutions of the materials according to the manufacturer's instructions (ThermoFisher Scientific). Briefly, BPs or their metabolites compete with a fluorescent ER ligand (tracer) for binding to the human ER α or β. The displacement of the tracer from the ER reduces fluorescent signal emission triggered by the excitation of conjugated terbium on the receptor. On the basis of the fluorescence loss, a dose–response curve was generated for each treated BP, and the half maximal inhibitory concentration (IC_{50}) was then calculated.

Nematode Chemical Exposure.

Caenorhabditis elegans nematodes were exposed to numbered and blinded samples of BPA, BPF, and BPAP as well as their degradation products following the protocol described previously.[32] Briefly, worm embryos were collected from the sensitized strain carrying the yIs34[*Pxol-1::GFP, rol-6*] reporter construct[32] by hypochlorite sodium treatment followed by L1 synchronization. L4 stage larvae were then transferred to M9 liquid culture buffer mixed with 100 μM of each BP or their degradation products for 24 h for a germline apoptosis assay (peak of germline morphology and function), and 48 h for fertility assessment (to maximize the number of impacted germ cells becoming embryos). Worms

were cultured with heat-inactivated bacteria as food in order to avoid potential bacterial metabolism of the compounds. New concentrated heat-inactivated bacteria were added at 24 h during the 48-h exposure to prevent food depletion.

Germline Apoptosis Assay.

After 24 h of exposure, as described above, worms were incubated with 25 μg/mL of acridine orange in M9 solution at room temperature for 2 h to stain the apoptotic nuclei in the germline as described previously.[33] After staining, the worms were transferred to new nematode growth media (NGM) plates for a 30 min recovery, and healthy worms were selected for microscopic examination. The total number of apoptotic nuclei in the posterior gonad of each worm was counted by fluorescence microscopy.

Fertility Assessment.

After 48 h of exposure, worms from each treatment group were individually transferred to new NGM plates without cholesterol and transferred every 12 h to a new plate. The numbers of eggs laid by each worm, larvae hatched from these eggs (i.e., embryonic lethality), and larvae successfully reaching adulthood (i.e., larval lethality) were tallied in the 3 days after exposure.

RESULTS

Characterization of vMnP.

The formation of rMnP and the vault complex was confirmed by Coomassie staining and Western blot analysis (Figure 1A). While by Coomassie staining vaults showed a clear band around 100 kDa, which is the size of MVP peptides forming vaults' shell, only rMnP was detectable by Western blot. Further examination with negative stain TEM revealed vMnP had identical morphology (Figure 1B) to the previously reported empty or INT bound vault nanoparticles.[12] The zeta potentials of empty vaults and vMnP were not significantly different (-20.50 ± 1.29 mV for empty vaults vs -18.65 ± 2.45 mV for vMnP, Figure 1C), indicating the incorporation of rMnP did not alter vaults' electrokinetic properties. The hydrodynamic diameters of empty and encapsulated vaults are both centered at 50 nm (Figure 1D), but more distribution at larger diameters was observed for vaults containing rMnP, implying the encapsulation of rMnP slightly up-shifted vault particles' hydrodynamic sizes. Additionally, the narrow distribution (45–65 nm) of both vaults also suggests that vault particles were uniformly dispersed.

Transformation of BPA.

Several 24-h time-course removal tests were performed using vMnP, rMnP, and nMnP, each with a low initial enzyme dosage at 19.3 U/L, which is 10–100 times lower than the dosage employed in previous peroxidase-catalyzed degradation studies.[2,22] As shown in Figure 2A, BPA concentration quickly dropped by 20–38% in the first 30 min. Afterward, nMnP and rMnP mediated BPA conversion stopped, and no further significant removal was observed. In contrast, BPA transformation under vMnP catalysis lasted for at least another 4 h. After 24 h, vMnP achieved approximately 96% removal of BPA, with negligible adsorption of

BPA on vaults, whereas only 42% and 25% BPA removals were observed for rMnP and nMnP, respectively (Figures 2A and S3).

BPA conversion mediated by vMnP followed pseudo-first-order kinetics for the first 4 h (Figure 2B), indicating there was no significant enzyme activity loss during this period. Between 4 and 24 h, the concentration of BPA further decreased from 10% to 4% of the initial concentration, indicating that vMnP still maintained activity. However, reactions no longer followed the pseudo-first-order kinetics. The alteration of BPA transformation kinetics was probably due to the competitive inhibition of vMnP by products formed by its activities, as over 90% of BPA was converted after 4 h and the resulting products were also favorable substrates of MnP enzymes.[2] For rMnP and nMnP, the pseudo-first-order conversion of BPA was only maintained for 30 min or less (Figure 2B insert). Figure 2C shows the change of nMnP mediated BPA conversion rates, which are calculated by normalizing concentration decreases to the intervals between two time points over the 24-h testing period. The rate peaked in the first 10 min to 113.0 μM/h and then rapidly decreased to near zero in 2 h. Similar results were also observed for rMnP, suggesting that both unencapsulated enzymes quickly lost their activities after initiating reactions and had significantly shorter lives under experimental conditions.

Next, we compared the performance of the three MnPs for removing BPA at different pHs in 24 h (Figure 2D). The results indicate that vMnP consistently showed better performance than unencapsulated rMnP and nMnP at pH 4.0, 4.5, and 5.0. However, due to fact that optimum pH for MnP is around 4, very low BPA removal was observed at pH 5.5. Therefore, these results validate that vMnP has longer functional longevity than nMnP and can still efficiently remove BPA at low enzyme dosage.

Transformation of BPA Analogues.

Although BPA has been progressively replaced in some commercial products, most of its substitutes are bisphenolic analogues that share a high degree of structural similarities, suggesting these alternatives may also be treatable by peroxidases. Therefore, we evaluated the effectiveness of vMnP for removing three widely used BPA analogues including BPS, BPF, and BPAP.[13]

Significant BPF and BPAP degradation was observed in the presence of each type of MnP tested, with BPF following very similar degradation kinetics compared to BPA (Figure S4A). After 24 h of reaction, the concentration of BPF decreased to 10.4% of its initial concentration for the vMnP treatment with no observed adsorption on vaults (Figure S3), while it only reached 53.7% and 64.4% after rMnP and nMnP treatments, respectively. For unencapsulated MnPs, most of the BPF removal occurred in the first hour, and no further concentration decrease was seen between 1 and 24 h, while vMnP-mediated BPF conversion increased from 50.2% to 64.8% between 1 and 3 h and finally reached 89.6% at 24 h. In the case of BPAP, only 19.0% degradation occurred by nMnP treatment, which is much lower than that of BPA and BPF, the rMnP mediated BPAP degradation reached 85.1% in 24 h (Figure S4B). Interestingly, vMnP exhibited slower BPAP conversion than rMnP in the first 6 h. About 81.0% BPAP removal was observed for rMnP after a 6-h reaction, while only 43.5% BPAP degradation was observed for vMnP. Due to its low solubility, BPAP forms

small aggregates when added into reaction solutions. These aggregates did not adsorb on vaults' surfaces (Figure S3) and had limited diffusion, thus the concentration of BPAP inside of the vaults was lower than in solution, and a very limited amount of BPAP was accessible to vMnP. Consistent with the lower diffusion of BPAP, we observed that over a longer incubation period (beyond 6 h) 74.7% removal was achieved. For rMnP, the degradation rate only increased by 4.1% between 6 and 24 h, indicating most of the enzyme activity was lost after a 6-h reaction. BPS was not degraded by any of the three MnPs within 24 h (Figure S5). Thus, the results of BPF and BPAP degradation further demonstrate that encapsulation of MnP in vaults significantly extends enzyme life in reactions and improves contaminant transformation efficiency.

Enzymatic Transformation Product Profiles.

Since vMnP and rMnP exhibited different degradation kinetics, we next characterized and compared the product profiles after vMnP and nMnP treatments for each BP. After SPE concentration, recoveries of parental bisphenolic compounds were over 90%, whereas high-molecular weight products (e.g., oligomers of bisphenolic compounds) may be recovered in lower yields because of their relatively lower solubility.[22] Concentrated products were then separated and analyzed by their retention times and mass-to-charge ratios (Figure 3) using UPLC/MS. This preliminary analysis indicates that vMnP and nMnP treatments generated significantly different product species as the reactions progressed. Referring to previously reported mechanisms of peroxidase catalyzed BPA transformation as well as products identified in this study,[2,22] the proposed MnP mediated reaction pathways for BPA, BPF, and BPAP are presented in Figures S6, S7, and S8, respectively. In general, the parent BPs undergo scission reactions that breakdown BPs to small-mass products, followed by coupling reactions that generate oligomeric BPs.

In the case of BPA, 17 and 24 products were detected after vMnP and nMnP treatments, respectively (Figure 3, left panel), most of which were not found in proposed MnP mediated BPA transformation (Figure S6). The encapsulated and unencapsulated forms of MnP enzyme shared only four common products. Among the 17 species identified for vMnP treatment, four (Figure S6, species A1–A4) were generated from proposed MnP catalysis, making up about 43.6% of the total MS response. For nMnP treatment, 24 species were identified, two of which were from the MnP catalyzed reaction (Figure S6, species A1 and A3), and accounted for only 9.1% of total MS response. The ion 133, which is the first intermediate in the proposed pathway, was reported at an abundance of 13.1% of the total MS response for vMnP as opposed to only 3.3% for nMnP. The next species in the pathway (Figure S6 species A2) was only found in the sample from vMnP treatment. BPA trimers or oligomers (Figure S6, species A4), which are formed at the end of the proposed pathway, exhibited an abundance of 10.1% of total MS response for vMnP, while those were not detected in the samples from rMnP treatment.

For BPF (Figure 3, middle panel), vMnP and nMnP treatments yielded more similar product profiles. Sixteen species were detected in the sample from vMnP treatment, five of which (Figure S7, species F1–F5) were from proposed MnP-mediated reactions and constituted about 81.0% of total MS response. For nMnP treatment, 23 species were identified, which

shared seven species with the vMnP treatment, four of which (Figure S7, species F1, F2, F3, and F4) were found in proposed enzymatic pathways and were about 60.0% of the total MS response. Product F2 (4-hydroxybenzaldehyde), which is the second product in MnP catalyzed BPF transformation pathways, was the most abundant species in both treatments, suggesting the subsequent reactions converting F2 may not be favored. Although species F1 and F2 were very abundant in both conditions, they still exhibited higher percentagesin the sample from vMnP treatment.

Finally, the product profiles of BPAP were more complex than those of BPA and BPF (Figure 3, right panel). Twenty-nine and thirty-two product species were identified for vMnP and nMnP treatments respectively, only six of which were shared between two enzymes. Five species (Figure S8, P1–P5) in the proposed enzymatic pathway were found from vMnP treatment, which accounted for about 33.8% of the total MS response, while only three were identified from nMnP treatment, making up for less than 8% of total MS response, which agrees with the findings for BPA and BPF. Together, these results imply that treatments by vMnP and nMnP resulted in significantly different product profiles, and transformation of BPs by vMnP fitted with proposed MnP-mediated pathways better than the transformation by nMnP.

Reduction in BPs' Toxicity.

Exposure to BPA has been associated with a variety of toxic responses including strong reproductive effects across a variety of organisms through mechanisms that are sometimes distinct from its weak affinity for the estrogen receptor (ER).[34–36] BPA's reproductive effects can be considered hallmarksof its toxicity as BPA exposure leads to a decrease in fertility that correlates with a decreased viability of germ cells in a great number of animal species examined to date, including humans and well-established laboratory model organisms such as mouse, rat, zebrafish, drosophila, and *C. elegans* worms.[25–30,37] The mechanisms underlying BPA's reproductive effects are also well conserved as BPA exposure was shown to cause an increase in germ cell death by apoptosis and an increase in chromosome errors and lethality in mouse and *C. elegans* early embryos.[25,27,30] In *C. elegans*, these findings were extended to the BPA analogue BPS, suggesting that the similarity in chemical structure imparts comparable effects on germ cells.[20] The remarkable conservation of reproductive toxicity outcomes caused by BPA exposure was leveraged here to examine whether MnP-mediated degradation of BPA and its analogues decreases their associated toxicity by monitoring the model organism *C. elegans*.

Following a single-blind protocol, we first examined the induction of germline apoptosis in the midpoint of the *C. elegans* gonad via acridine orange staining. Following exposure to BPA and BPF at a reference concentration of 100 μM for 24 h spanning the onset of reproduction (L4 to adult), we observed a significant 40% to 60% increase in the number of apoptotic nuclei when compared to the 0.1% ethanol vehicle control ($P \leq 0.05$, Student's *t* test; Figure 4). A similar significant increase was observed in the enzyme-free/mock treatment group. In contrast, vMnP treatment dramatically reduced the BPA, BPF, and BPAP-mediated germline apoptosis effect to levels indistinguishable from controls. The

results were more variable for the nMnP as BPA and BPF degradation did not reduce their impacts on germline apoptosis while it did for the BPAP group.

Next, we assessed the impactsof the various treatments on BPA, BPF, and BPAP-induced embryonic lethality (Figure 5). Compared to the control, both BPA and BPAP exposure significantly increased the embryonic lethality by 48% and 38%, respectively ($P \leq 0.05$, student's t test), while BPF exposure induced a 19% increase but failed to reach a statistical significance. Among all treatment groups—enzyme free/mock, nMnP, and vMnP—only the latter led to a reduction in embryonic lethality to a level comparable to controls. The stronger reduction in germline apoptosis compared to embryonic lethality can be explained by the fact that the solvent using 0.1% ethanol alone causes some degree of embryonic lethality and therefore increased the baseline of the lethality assay (Figure S9). However, the embryonic results are particularly significant considering that no effect of any of the BPs was detected on later stages of the nematode's development as measured by larval survival assay (Figure S10).

The dramatic decrease in the BPs' reproductive toxicity after vMnP treatment could be due to a reduction in their estrogenic activity. To test this possibility, we assessed the ability of nMnP and vMnP to decrease the association of BPA, BPF, and BPAP with the estrogen receptors α and β following treatment using a fluorescence displacement assay. After 24 h, both nMnP- and vMnP-mediated transformation products showed a decreased ability to bind the ERs for all tested BPs (Figure S11). Interestingly, vMnP exhibited better performance toward reducing BPAP ER binding while nMnP displayed a preference toward BPA and BPF. However, taken together, these results highlight the successful detoxification of BPA, BPF, and BPAP by vMnP.

DISCUSSION

Application of white-rot fungi for removing organic micro-contaminants in water is becoming increasingly feasible.[3] As one of the major components in the extracellular enzymatic machinery of white-rot fungi, MnP is capable of degrading a wide variety of contaminants and has great potential in water treatment. By encapsulating MnP into vault nanoparticles, we observed significant improvement of BPA, BPF, and BPAP removal and a remarkable decrease in reproductive toxicity of degradation products.

The removal efficiencies of four tested BPs were ranked as BPA ≈ BPF > BPAP ≫ BPS, and vMnP showed higher removal rates than nMnP for all compounds except for BPS. The absence of BPS degradation was somewhat unexpected since it has two phenolic hydroxyl groups that are appropriate targets for MnP. However, similar results were also reported in a study testing natural attenuation of BPS in seawater,[38] which showed significant biodegradation of BPA and BPF but not of BPS. One possible explanation is that the sulfonyl group that connects two phenol functional groups makes BPS more electronegative (Table S1), thus BPS tends to serve as an electron acceptor rather than donor. It is supported by a study comparing biodegradation of various BPs under aerobic and anaerobic conditions, which showed that BPS was highly tolerant against aerobic biodegradation but was more susceptible to anaerobic biodegradation.[39]

Comparing vMnP to nMnP in removing BPA, BPF, and BPAP, vMnP exhibited significantly higher transformation rates and extended functional longevity. To reduce the cost of enzyme usage and provide a cost-effective enzymatic treatment approach, we employed 10–100 times lower enzyme dosage than other studies,[2,22] thus limited removal was observed using nMnP. It only lasted 0.5–1 h in reactions, which was notably shorter than its storage life. This result is in good agreement with a previous study on BPA removal by free horseradish peroxidase,[22] which showed that BPA concentration decreased rapidly in the first 3–5 min and then gradually leveled off between 5 and 30 min. The rapid enzyme inactivation can be attributed to the attack from H_2O_2,[1,40] heme disruption caused by phenolic radicals,[41] or heat inactivation.[8] By encapsulating in vaults, enzymatic longevity in reactions was substantially improved (at least five folds during BPA degradation), which attests that vault encapsulation not only stabilizes enzymes during storage[8] but also protects them from H_2O_2 and radical attack. The mechanism is not clear, but one possible way is to prevent heme release by hindering enzymatic conformation change upon attack.[4]

The distinct production of transformation products of each BP between vMnP and nMnP treatments is also attributed to their different stability in reactions. With enhanced functional longevity, vMnP-mediated BPs transformation accorded more closely with proposed MnP catalytic mechanism (Figures S6, S7, and S8), while the less stable nMnP resulted in different products, the majority of which were not mapped to proposed MnP-mediated pathways. It is possible that BP transformation intermediates that were formed by MnP activities were chemically transformed by oxidizing agents in the system, such as H_2O_2, which also contributed to the final product pool. For nMnP, the enzyme only survived long enough to convert BPA, BPF, and BPAP to the initial intermediates, as it was inactivated rapidly in the reactions. Afterward, these initial intermediates were transformed mostly via chemical reactions, forming the majority of the detected products, which are not in the general enzymatic transformation pathways (Figures S6, S7, and S8). For instance, in nMnP mediated BPA transformation, the species with an m/z of 181 is probably a product from chemical oxidation of A1 (Figure S6) at the phenoxy group.[42] In contrast, vMnP lasted much longer in the reactions, which allowed the continued transformation to downstream products, such as BPA trimers or oligomers, which are relatively inert to chemical reactions and less toxic as discussed in detail below. Additionally, vMnP catalyzed reactions also consumed H_2O_2 and, thus, further reduced the likelihood of direct chemical oxidation.

Finally, vMnP treatment significantly reduced the toxicity of the BPs tested, unlike nMnP treatment. For this purpose, we used the nematode *C. elegans* because of its tractability, short reproductive period, conservation of reproductive pathways, and of reprotoxicity response to BPA.[20,25] Interestingly, we found that the ability of BPA and BPF to increase the germline apoptosis was eliminated by vMnP treatment but not by nMnP. As compared to nMnP, vMnP was more efficient in reducing the fertility impact of BPA and BPAP on nematodes. These results corroborate that vMnP not only efficiently removes the parent BPs from solution but also leads to the production of reaction intermediates and final products that are altogether less reprotoxic than the parent compounds. Divergence between vMnP and nMnP in decreasing estrogenic activity of BPs was also noted. We attribute these differences to the distinct enzymatic kinetics with differing final product profiles. The partial overlap between the reprotoxicity assays and the ER binding assay is supported by

the literature on BPA which shows that BPA-induced reproductive effects only partially correlate with its described weak estrogenic affinity.[34–36] Altogether, these experiments highlight the utility and sensitivity of the reproductive end points in *C. elegans*, which can therefore serve to assess the efficacy of various water treatment strategies.

Previous studies on advanced oxidation of BPA showed that the product toxicity is highest at earlier time points, which was attributed to the accumulation of initial oxidation intermediates.[23,24] It is believed that these initial intermediates are more toxic, while higher-molecular weight intermediates such as BPA dimers, trimers, or oligomers are relatively less toxic. In this study, although very low amounts of initial intermediates in the enzymatic pathway were detected for nMnP, it is possible that these compounds were chemically converted to structurally similar compounds, which still possess reproductive toxicity. For the vMnP system, a significant amount of BP oligomers was detected, indicating the conversion of initial intermediates to less toxic polymeric products via the enzymatic pathway. Thus, our results imply that this difference in product profiles might underlie the remarkable amelioration of BPs' toxicity following vMnP treatment.

This study evaluated the use of vault nanoparticle-encapsulated MnP enzymes as an effective water treatment approach and assessed the health risk of treatment products using a combination of *in vivo* and *in vitro* assays. It was demonstrated that vault encapsulation enhances enzymatic functional longevity in reactions and lowers the enzyme dosage requirement for effective removal of bisphenolic water contaminants. The reduction in BPA, BPF, and BPAP's reproductive toxicity in the nematode *C. elegans* following vMnP treatment aligns with their efficient removal after 24 h and confirms that the process does not generate significant amounts of degradation products that also carry reproductive toxicity. Therefore, enzyme stabilization in vault nanoparticles combined with rigorous assessment of product toxicity opens up an exciting perspective toward the application of safe and sustainable enzymatic systems for the treatment of BPs in water. Co-encapsulation of multiple enzymes involved in transformation of several contaminants will expand the applicability of the vault-encapsulated enzyme systems for removing a suite of contaminants in natural and engineered systems. Furthermore, the vault particle provides a manipulation platform that can be readily embedded in membrane reactors or filtration units, which allows easy reuse of the encapsulated enzymes and facilitates their applications in water treatment processes and point-of-use devices.

Supplementary Material

Refer to Web version on PubMed Central for supplementary material.

ACKNOWLEDGMENTS

This research was supported by Strategic Environmental Research and Development Program (SERDP) Award ER2422, R01 NIH/NIEHS ES02748701, the Burroughs Wellcome Foundation, and UCLA Department of Civil and Environmental Engineering. Y.C. received support from the T32 NIH/NIEHS ES015457 Training in Molecular Toxicology. S.M. received the 2017 Paul L. Busch Award from The Water Research Foundation. The authors thank Dr. G. Khitrov for assistance with UPLC/MS analysis.

REFERENCES

(1). Franssen MCR; Steunenberg P; Scott EL; Zuilhof H; Sanders JPM Immobilised enzymes in biorenewables production. Chem. Soc. Rev 2013, 42, 6491–6533. [PubMed: 23519171]

(2). Hirano T; Honda Y; Watanabe T; Kuwahara M Degradation of bisphenol A by the lignin-degrading enzyme, manganese peroxidase, produced by the white-rot basidiomycete, Pleurotus ostreatus. Biosci., Biotechnol., Biochem 2000, 64 (9), 1958–1962. [PubMed: 11055402]

(3). Mir-Tutusaus JA; Baccar R; Caminal G; Sarrà M Can white-rot fungi be a real wastewater treatment alternative for organic micropollutants removal? A review. Water Res 2018, 138, 137–151. [PubMed: 29579480]

(4). Wei W; Du JJ; Li J; Yan M; Zhu Q; Jin X; Zhu XY; Hu ZM; Tang Y; Lu YF Construction of robust enzyme nanocapsules for effective organophosphate decontamination, detoxification, and protection. Adv. Mater 2013, 25 (15), 2212–2218. [PubMed: 23436305]

(5). Cipolatti EP; Valério A; Henriques RO; Moritz DE; Ninow JL; Freire DMG; Manoel EA; Fernandez-Lafuente R; de Oliveira D Nanomaterials for biocatalyst immobilization – state of the art and future trends. RSC Adv 2016, 6, 104675–104692.

(6). Meryam Sardar RA Enzyme Immobilization: An overview on nanoparticles as immobilization matrix. Biochem. Anal. Biochem 2015, 4, 148.

(7). Polka JK; Hays SG; Silver PA Building spatial synthetic biology with compartments, scaffolds, and communities. Cold Spring Harbor Perspect. Biol 2016, 8 (8), a024018.

(8). Wang M; Abad D; Kickhoefer VA; Rome LH; Mahendra S Vault nanoparticles packaged with enzymes as an efficient pollutant biodegradation technology. ACS Nano 2015, 9 (11), 10931–10940. [PubMed: 26493711]

(9). Rome LH; Kickhoefer VA Development of the vault particle as a platform technology. ACS Nano 2013, 7 (2), 889–902. [PubMed: 23267674]

(10). Stephen AG; Raval-Fernandes S; Huynh T; Torres M; Kickhoefer VA; Rome LH Assembly of vault-like particles in insect cells expressing only the major vault protein. J. Biol. Chem 2001, 276 (26), 23217–23220. [PubMed: 11349122]

(11). Wang M; Kickhoefer VA; Rome LH; Foellmer OK; Mahendra S Synthesis and assembly of human vault particles in yeast. Biotechnol. Bioeng 2018, 115 (12), 2941–2950. [PubMed: 30171681]

(12). Kickhoefer VA; Garcia Y; Mikyas Y; Johansson E; Zhou JC; Raval-Fernandes S; Minoofar P; Zink JI; Dunn B; Stewart PL; Rome LH Engineering of vault nanocapsules with enzymatic and fluorescent properties. Proc. Natl. Acad. Sci. U. S. A 2005, 102 (12), 4348–4352. [PubMed: 15753293]

(13). Liao CY; Liu F; Moon HB; Yamashita N; Yun SH; Kannan K Bisphenol analogues in sediments from industrialized areas in the United States, Japan, and Korea: spatial and temporal distributions. Environ. Sci. Technol 2012, 46 (21), 11558–11565. [PubMed: 23020513]

(14). Chen MY; Ike M; Fujita M Acute toxicity, mutagenicity, and estrogenicity of bisphenol-A and other bisphenols. Environ. Toxicol 2002, 17 (1), 80–86. [PubMed: 11847978]

(15). Pivnenko K; Pedersen GA; Eriksson E; Astrup TF Bisphenol A and its structural analogues in household waste paper. Waste Manage 2015, 44, 39–47.

(16). Guo HY; Li H; Liang N; Chen FY; Liao SH; Zhang D; Wu M; Pan B Structural benefits of bisphenol S and its analogs resulting in their high sorption on carbon nanotubes and graphite. Environ. Sci. Pollut. Res 2016, 23 (9), 8976–8984.

(17). Han J; Cao Z; Qiu W; Gao W; Hu JY; Xing BS Probing the specificity of polyurethane foam as a ‘solid-phase extractant’: Extractability-governing molecular attributes of lipophilic phenolic compounds. Talanta 2017, 172, 186–198. [PubMed: 28602294]

(18). Yamazaki E; Yamashita N; Taniyasu S; Lam J; Lam PKS; Moon HB; Jeong Y; Kannan P; Achyuthan H; Munuswamy N; Kannan K Bisphenol A and other bisphenol analogues including BPS and BPF in surface water samples from Japan, China, Korea and India. Ecotoxicol. Environ. Saf 2015, 122, 565–572. [PubMed: 26436777]

(19). Lee S; Liao C; Song GJ; Ra K; Kannan K; Moon HB Emission of bisphenol analogues including bisphenol A and bisphenol F from wastewater treatment plants in Korea. Chemosphere 2015, 119, 1000–1006. [PubMed: 25303660]

(20). Chen YC; Shu L; Qiu ZQ; Lee DY; Settle SJ; Que Hee S; Telesca D; Yang X; Allard P Exposure to the BPA-substitute bisphenol S causes unique alterations of germline function. PLoS Genet 2016, 12 (7), No. e1006223.

(21). Audebert M; Dolo L; Perdu E; Cravedi JP; Zalko D Use of the γH2AX assay for assessing the genotoxicity of bisphenol A and bisphenol F in human cell lines. Arch. Toxicol 2011, 85 (11), 1463–1473. [PubMed: 21656223]

(22). Huang QG; Weber WJ Transformation and removal of bisphenol A from aqueous phase *via* peroxidase-mediated oxidative coupling reactions: efficacy, products, and pathways. Environ. Sci. Technol 2005, 39 (16), 6029–6036. [PubMed: 16173560]

(23). Lu N; Lu Y; Liu FY; Zhao K; Yuan X; Zhao YH; Li Y; Qin HW; Zhu J $H_3PW_{12}O_{40}/TiO_2$ catalyst-induced photo-degradation of bisphenol A (BPA): kinetics, toxicity and degradation pathways. Chemosphere 2013, 91 (9), 1266–1272. [PubMed: 23540812]

(24). Olmez-Hanci T; Arslan-Alaton I; Genc B Bisphenol A treatment by the hot persulfate process: oxidation products and acute toxicity. J. Hazard. Mater 2013, 263, 283–290. [PubMed: 23433897]

(25). Allard P; Colaiacovo MP Bisphenol A impairs the doublestrand break repair machinery in the germline and causes chromosome abnormalities. Proc. Natl. Acad. Sci. U. S. A 2010, 107 (47), 20405–20410. [PubMed: 21059909]

(26). Chen J; Saili KS; Liu Y; Li L; Zhao Y; Jia Y; Bai C; Tanguay RL; Dong Q; Huang C Developmental bisphenol A exposure impairs sperm function and reproduction in zebrafish. Chemosphere 2017, 169, 262–270. [PubMed: 27880925]

(27). Hunt PA; Koehler KE; Susiarjo M; Hodges CA; Ilagan A; Voigt RC; Thomas S; Thomas BF; Hassold TJ Bisphenol A exposure causes meiotic aneuploidy in the female mouse. Curr. Biol 2003, 13 (7), 546–553. [PubMed: 12676084]

(28). Kato H; Furuhashi T; Tanaka M; Katsu Y; Watanabe H; Ohta Y; Iguchi T Effects of bisphenol A given neonatally on reproductive functions of male rats. Reprod. Toxicol 2006, 22 (1), 20–29. [PubMed: 16311018]

(29). Li DK; Zhou Z; Miao M; He Y; Wang J; Ferber J; Herrinton LJ; Gao E; Yuan W Urine bisphenol-A (BPA) level in relation to semen quality. Fertil. Steril 2011, 95 (2), 625–630. [PubMed: 21035116]

(30). Susiarjo M; Hassold TJ; Freeman E; Hunt PA Bisphenol A exposure in utero disrupts early oogenesis in the mouse. PLoS Genet 2007, 3 (1), No. e5.

(31). Kar UK; Srivastava MK; Andersson A; Baratelli F; Huang M; Kickhoefer VA; Dubinett SM; Rome LH; Sharma S Novel CCL21-vault nanocapsule intratumoral delivery inhibits lung cancer growth. PLoS One 2011, 6 (5), No. e18758.

(32). Allard P; Kleinstreuer NC; Knudsen TB; Colaiacovo MP A *C. elegans* screening platform for the rapid assessment of chemical disruption of germline function. Environ. Health Perspect 2013, 121 (6), 717–724. [PubMed: 23603051]

(33). Gartner A; Boag PR; Blackwell TK Germline survival and apoptosis. In WormBook; The C. elegans Research Community, 2008; pp 1–20, DOI: 10.1895/wormbook.1.145.1.

(34). Maffini MV; Rubin BS; Sonnenschein C; Soto AM Endocrine disruptors and reproductive health: the case of bisphenol-A. Mol. Cell. Endocrinol 2006, 254–255, 179–186.

(35). Rubin BS Bisphenol A: an endocrine disruptor with widespread exposure and multiple effects. J. Steroid Biochem. Mol. Biol 2011, 127 (1–2), 27–34. [PubMed: 21605673]

(36). Vandenberg LN; Hauser R; Marcus M; Olea N; Welshons WV Human exposure to bisphenol A (BPA). Reprod. Toxicol 2007, 24 (2), 139–177. [PubMed: 17825522]

(37). Atli E The effects of three selected endocrine disrupting chemicals on the fecundity of fruit fly, Drosophila melanogaster. Bull. Environ. Contam. Toxicol 2013, 91 (4), 433–437. [PubMed: 23963441]

(38). Danzl E; Sei K; Soda S; Ike M; Fujita M Biodegradation of bisphenol A, bisphenol F and bisphenol S in seawater. Int. J. Environ. Res. Public Health 2009, 6 (4), 1472–1484. [PubMed: 19440529]

(39). Ike M; Chen MY; Danzl E; Sei K; Fujita M Biodegradation of a variety of bisphenols under aerobic and anaerobic conditions. Water Sci. Technol 2006, 53 (6), 153–159.

(40). Wariishi H; Akileswaran L; Gold MH Manganese peroxidase from the basidiomycete *Phanerochaete chrysosporium*: spectral characterization of the oxidized states and the catalytic cycle. Biochemistry 1988, 27 (14), 5365–5370. [PubMed: 3167051]

(41). Mao L; Luo SQ; Huang QG; Lu JH Horseradish peroxidase inactivation: heme destruction and influence of polyethylene glycol. Sci. Rep 2013, 3, 3126. [PubMed: 24185130]

(42). Zazo JA; Casas JA; Mohedano AF; Gilarranz MA; Rodriguez JJ Chemical pathway and kinetics of phenol oxidation by Fenton's reagent. Environ. Sci. Technol 2005, 39 (23), 9295–9302. [PubMed: 16382955]

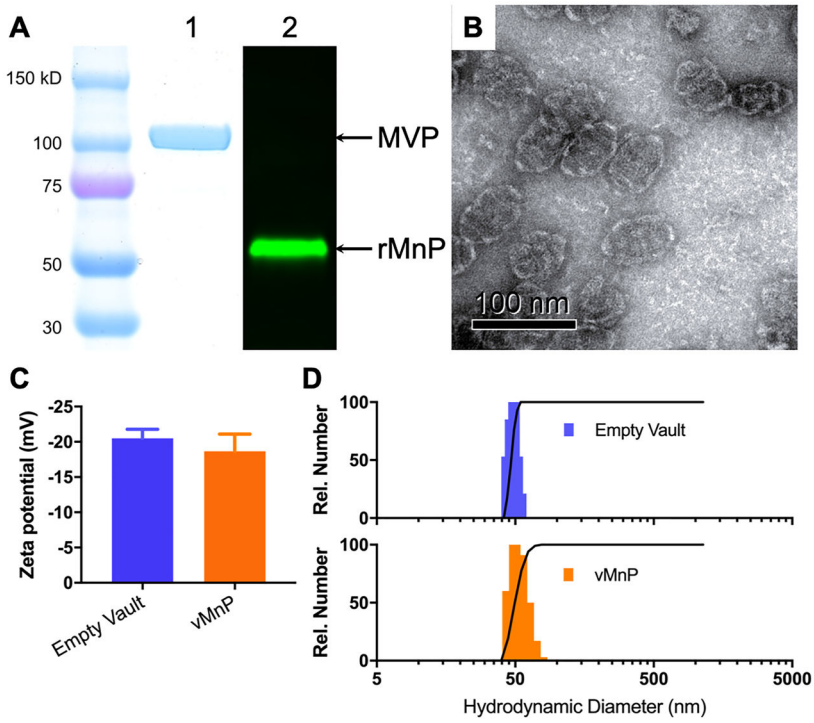

Figure 1.

Characterization of vMnP. (A) vMnP was fractionated on a 4–15% SDS-PAGE and analyzed by Coomassie staining (lane 1) and Western blotting using anti-INT antibody (lane 2). MVP and rMnP bands are indicated by arrows. (B) Negative-stained TEM image of vMnP. (C) Comparison of aeta potentials of empty vaults and vMnP. Error bars represent one standard error of the mean ($n = 10$). (D) Number-based distribution of hydrodynamic diameters of empty vaults and vMnP.

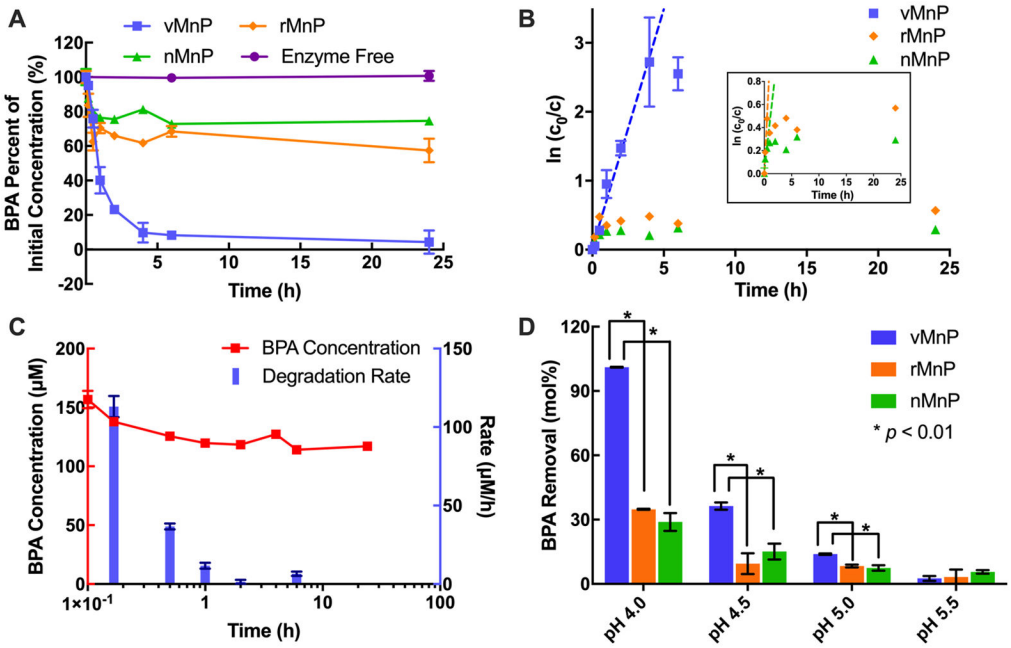

Figure 2.

Enhanced BPA removal by vMnP. (A) Removal of BPA mediated by vMnP, rMnP, and nMnP. In 24 h, vMnP degraded nearly 100% of BPA, as compared with only 30–40% BPA degradation by rMnP and nMnP enzymes. (B) Pseudo-first-order kinetics of BPA transformation. vMnP mediated BPA transformation followed pseudo-first-order kinetics in the first 4 h, but nMnP- and rMnP-driven BPA conversion only obeyed the kinetics for the first 30 min. (C) nMnP mediated BPA conversion rates. The rate of nMnP-catalyzed BPA removal immediately decreased after initiating reaction. (D) Vault encapsulation enhanced BPA removal at various pHs. Error bars represent one standard error of the mean ($n = 3$).

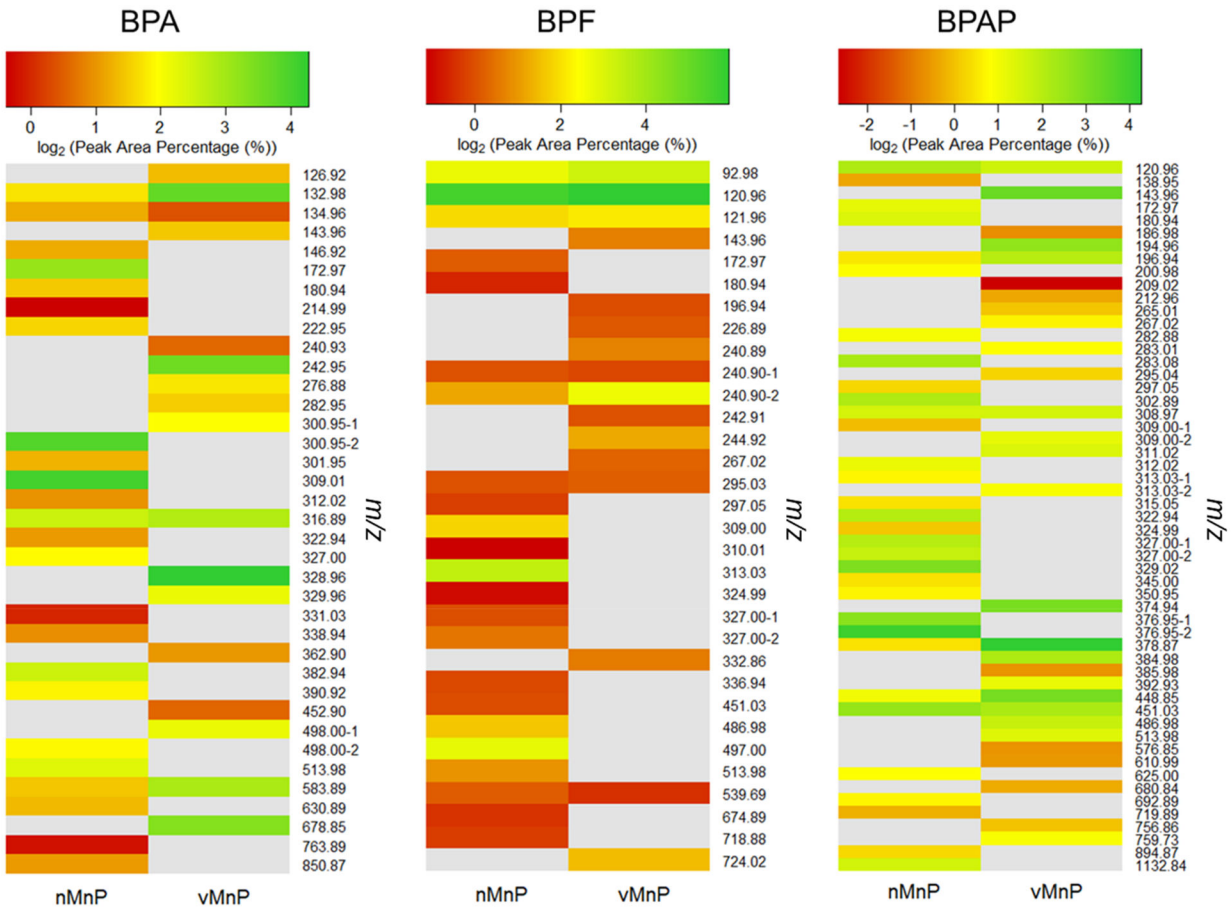

Figure 3.

Comparison of product profiles among vMnP and nMnP treatments for BPA, BPF, and BPAP. Products were separated and named by their UPLC retention time and mass-to-charge ratios (*m*/*z*) and plotted based on their relative abundance. Treatments by vMnP and nMnP generated significant different products. Gray color indicates that the ion was not detected in the sample.

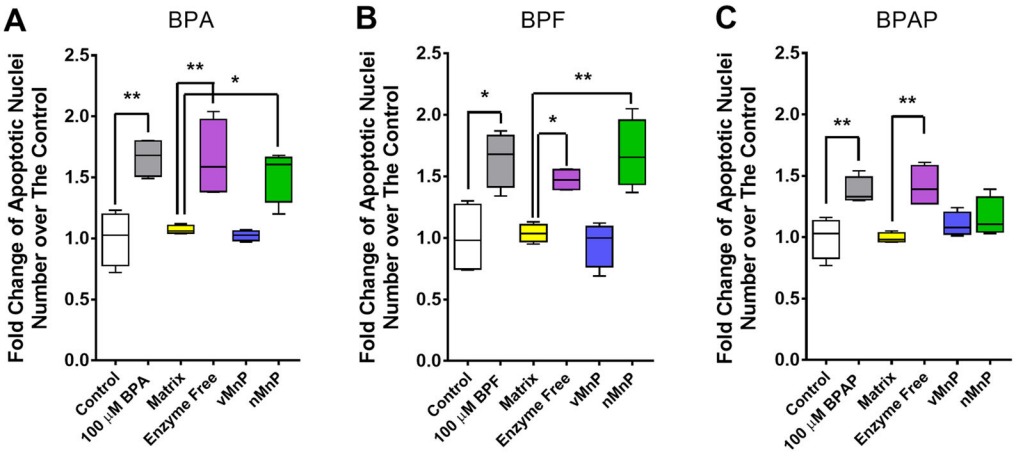

Figure 4.

Germline apoptosis of worms exposed to BPs and their biodegradation products. As compared to vehicle control (0.1% ethanol), 24 h exposure to 100 μM of BPA (A), BPF (B), or BPAP (C) significantly increased apoptotic germline nuclei numbers by 66%, 64%, and 38%, respectively. The increase in germline apoptosis was also observed in the mock BPs groups with no treatment (Enzyme Free), as well as the nMnP treated BPA and BPF groups. In contrast, biodegradation mediated by vMnP completely removed the ability of BPA, BPF, and BPAP to induce germline apoptosis compared to the Matrix control (no chemical). Student's *t* test performed for the comparison between the control and each 100 μM bisphenol group. One way-ANOVA with posthoc Tukey HSD test performed for the comparison among all BPs treatment groups. $*P < 0.05$ and $**P < 0.01$. $N = 4$.

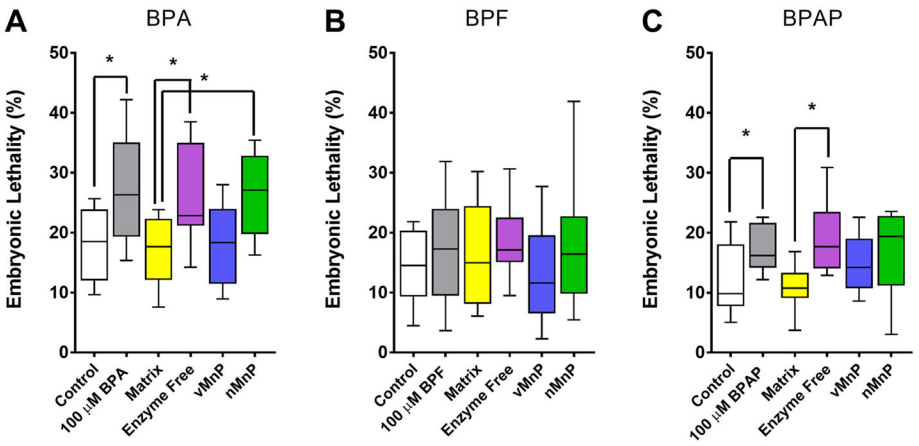

Figure 5.

Embryonic lethality of BPs and their biodegradation products. Embryonic lethality is calculated as the percentage of unhatched eggs in all the eggs laid by each worm. Compared with the vehicle control (0.1% ethanol), exposure to 100 μM BPA (A) or BPAP (C) significantly increases the embryonic lethality by 48% and 38%, respectively, while 100 μM BPF (B) showed a 22% increase but failed to reach statistical significance. After the biodegradation reaction, vMnP, but not nMnP, BP treatment led to a reduction in embryonic lethality to a level comparable to the buffer control group (Matrix). Student's *t* test performed for the comparison between the control and each 100 μM bisphenol group. One way-ANOVA with posthoc Tukey HSD test performed for the comparison among all BPs treatment groups. $*P < 0.05$. $N = 10–13$.